Temporal Variation of Scour Depth at Nonuniform Cylindrical Piers

Jau-Yau Lu, M.ASCE[1]; Zhong-Zhi Shi[2]; Jian-Hao Hong[3]; Jun-Ji Lee, Ph.D.[4]; and Rajkumar V. Raikar[5]

Abstract: The paper proposes a semiempirical model to estimate the temporal development of scour depth at cylindrical piers with unexposed foundations. A cylindrical pier with a foundation is considered as nonuniform pier. The concept of primary vortex and the principle of volumetric rate of sediment transport are used to develop a methodology to characterize the rate of evolution of the scour hole at nonuniform cylindrical piers. The model also simulates the entire scouring process at nonuniform cylindrical piers having the discontinuous surface located below the initial bed level. The scouring process includes three zones; viz Zone 1 having the scouring phenomenon similar to that of a uniform pier, Zone 2 in which the scour depth remains unchanged with its value equal to the depth of the top level of foundation below the initial bed level while the dimensions of the scour hole increase, and in Zone 3 the geometry pier foundation influences the scouring process. A concept of superposition using an effective pier diameter is proposed to simulate the scouring process in Zone 3. In addition, the laboratory experiments were conducted to utilize the laboratory results for the validation of the model. The simulated results obtained from the proposed model are in good agreement with the present experimental results and also other experimental data. Also, the effect of unsteadiness of flow is incorporated in the model and the results of the model are compared with the experimental data. The model agrees satisfactorily with the experimental data.

DOI: 10.1061/(ASCE)HY.1943-7900.0000272

CE Database subject headings: Bridges; Piers; Steady flow; Unsteady flow; Time dependence; Scour; Sediment transport.

Author keywords: Bridge pier; Nonuniform pier; Steady flow; Unsteady flow; Time dependence; Scour; Sediment transport.

Introduction

The failure of bridges due to excessive local scour during floods poses a challenging problem to hydraulic engineers. Scour at bridge locations is a complex phenomenon caused by various agents such as localized scour combined with general riverbed degradation, modification of flow field around bridge structures, human interference, debris flow, etc. However, it is reported that the formation of three-dimensional vortex flow field around the pier (e.g., Keutner 1932; Shen et al. 1969; Dey et al. 1995) consisting of horseshoe vortex is primarily responsible for the scour at bridge piers. Out of 823 bridge failures in the United States since 1951, it was reported that 60% of bridge failures were caused by the effects of hydraulics that include channel instability and bridge pier scour (Shirhole and Holt 1991). Therefore, the study on the phenomena of pier scour has become a topic of continued interest to the investigators. After the pioneering work of Durand-Claye (1873) on the investigation of pier scour, numerous investigations on pier scour have been reported by various researchers. Review of the important experiments and field studies was given by Breusers et al. (1977); Dargahi (1982); Breusers and Raudkivi (1991); Dey (1997a,b); Hoffmans and Verheij (1997); Melville and Coleman (2000); and Richardson and Davis (2001).

Most of the investigations reported in the aforementioned reviews were done on the scour process at a uniform pier. However, in reality many bridge piers behave as nonuniform depending on the exposure of their foundation into the flow field. It depends on the evolution of scour hole, which is a factor of pier geometry, flow characteristics, and bed material properties. In the present study, a cylindrical pier with a foundation is considered as nonuniform pier. Therefore, the temporal variation of scour depth at nonuniform piers is a topic of important research because the time factor may play a significant role in the determination of the closure time for cross-river bridges. Numerous time variation models for the estimation of scour depth at uniform piers were developed by various investigators (Shen et al. 1965; Johnson and McCuen 1991; Yanmaz and Altinbilek 1991; Kothyari et al. 1992; Sumer et al. 1992; Dey 1999; Mia and Nago 2003, Chang et al. 2004; Oliveto and Hager 2005). On the other hand, Imamoto and Ohtoshi (1987) developed a numerical model to simulate the temporal variation of the scour at a nonuniform cylindrical pier with a protruding foundation. However, their model was not tested with the experimental results. Furthermore, the detailed experimental investigations on the scouring process at the nonuniform piers were reported by Melville and Raudkivi (1996) and Oliveto et al. (2005).

Thus, the development of a model for the temporal variations

[1]Professor, Dept. of Civil Engineering, National Chung Hsing Univ., Taichung 402, Taiwan, Republic of China (corresponding author). E-mail: jylu@mail.nchu.edu.tw

[2]Senior Graduate Student, Dept. of Civil Engineering, National Chung Hsing Univ., Taichung 402, Taiwan, Republic of China.

[3]Postdoctoral Research Fellow, Dept. of Civil Engineering, National Chung Hsing Univ., Taichung 402, Taiwan, Republic of China.

[4]Dept. of Civil Engineering, National Chung Hsing Univ., Taichung 402, Taiwan, Republic of China.

[5]Professor, Dept. of Civil Engineering, K. L. E. S. College of Engineering and Technology, Belgaum 590008, India.

Note. This manuscript was submitted on September 1, 2009; approved on April 27, 2010; published online on May 1, 2010. Discussion period open until June 1, 2011; separate discussions must be submitted for individual papers. This paper is part of the ***Journal of Hydraulic Engineering***, Vol. 137, No. 1, January 1, 2011. ©ASCE, ISSN 0733-9429/2011/1-45–56/$25.00.

of scour depths at nonuniform piers with unexposed foundations is the topic of utmost importance. This paper presents a semi-empirical model developed to estimate the temporal variation of scour depth at nonuniform piers with unexposed foundations using the concept of the primary vortex and the sediment transport theory. The methods proposed by Mia and Nago (2003) and Melville and Raudkivi (1996) are combined to simulate the scouring process in front of a pier with the effect of foundation geometry. Furthermore, for unsteady flow with clear-water scour conditions, the model is extended for the nonuniform piers incorporating different flood hydrographs. In addition, experiments were carried out to validate the model using laboratory results.

Experimental Setup and Procedure

The laboratory experiments were carried out in a 17-m-long glass-sided rectangular flume having a cross section of 0.6 m wide and 0.6 m deep at the Department of Civil Engineering, National Chung Hsing University, Taichung, Taiwan. The pier models made of plexiglass were embedded vertically in the middle of the sand recess of 7.5 m long, 0.6 m wide, and 0.25 m deep, which retained uniform sand of median size, $d_{50} = 0.52$ mm, having geometrical standard deviation σ_g of less than 1.4. The test section was located approximately at 10 m downstream of the flume entrance. The flow straighteners fitted at the upstream end of the flume facilitated in producing a nearly uniform approaching flow. The false floor was constructed at an elevation of 0.25 m from the flume bottom throughout the length of the flume in order to provide the same bed level as that of the sand level in the recess. The top surface of the false floor was glued with the same uniform sand that was used in the experiments. All the experiments were run under clear-water scour conditions ($U/U_c < 1$, where U=average approaching flow velocity and U_c=critical velocity) with the approaching flow depth h being controlled by the tailgate. The average approaching flow velocity was determined from the vertical velocity profile measured at the centerline of the flume 2 m upstream of the pier by an acoustic Doppler velocimeter. The critical velocity U_c was calculated using the equation of semilogarithmic average velocity, as was done by Chiew (1984). As $U/U_c \leq 0.9$ in the present study, no significant dunes were observed in the approaching bed even though sand size used was having $d_{50}=0.52$ mm. Furthermore, based on the bed form discrimination proposed by Simons and

Table 1. Experimental Data under Steady-Flow Conditions [Present Study and Melville and Raudkivi (1996)]

Run	D (mm)	D^* (mm)	Z (mm)	h (mm)	U/U_c (—)	t_e (min)	Observed d_{se} (mm)	Computed d_{se} (mm)
(a) Present study ($d_{50}=0.52$ mm)								
S1	35	50	50	204	0.9	5,024	55	68.7
S2	35	50	35	204	0.9	4,975	74	62.1
S3	35	50	25	204	0.9	4,455	78	58.2
S4	20	50	10	204	0.9	3,124	26	37.3
S5	35	50	25	197	0.8	5,400	34	36.8
S6	50	70	30	204	0.9	3,323	96	94.4
S7	50	70	30	186	0.7	2,809	45	40.8
S8	50	70	20	204	0.9	5,631	110	109
S9	50	70	20	179	0.65	2,821	37	29.2
S10	50	70	10	204	0.9	3,995	108	126
S11	50	70	10	179	0.65	5,340	42	31
(b) Melville and Raudkivi (1996) ($d_{50}=0.8$ mm)								
MR-D1	30	81	35	200	1.0	—	38	53
MR-D2	30	81	30	200	1.0	—	42	53
MR-D3	30	81	25	200	1.0	—	65	53.5
MR-D4	45	63	70	200	1.0	—	85	85.8
MR-D5	45	63	60	200	1.0	—	95	101
MR-D6	45	63	30	200	1.0	—	98	66.78
MR-D7	45	81	70	200	1.0	—	73	70
MR-D8	45	81	60	200	1.0	—	76	71
MR-D9	45	81	40	200	1.0	—	89	71
MR-D10	30	81	50	200	1.0	—	50	50
MR-D11	25	81	30	200	1.0	—	30	30
MR-D12	25	81	20	200	1.0	—	57	47
MR-D13	45	55	45	200	1.0	—	96	87.7
MR-D14	30	63	45	200	1.0	—	45	45
MR-D15	30	63	38	200	1.0	—	50	71
MR-D16	30	63	30	200	1.0	—	56	59
MR-D17	30	63	25	200	1.0	—	62	53.9
MR-D18	10	81	20	200	1.0	—	20	19.3

Note: "—" denotes data not available.

Richardson (1966) and Shields-Parkers river sedimentation diagram (García 2008), all the experiments conducted belong to no motion conditions for the approaching mobile bed. The temporal evolution of scour depth at the pier nose was measured with a periscope (accuracy of the periscope is 0.5 mm) inserted in the pier, while the water surface elevation was determined by a vernier point gauge.

To remove the entrapped air from the sediment recess, the flume was initially filled with water and left undisturbed for approximately 24 h. Before the experimental run being started, the flume was filled with water from the downstream end until the flow depth reaches the desirable value, which would help in avoiding the undesirable scour by the action of sheet flow. Then the flow discharge was gradually increased to the required value corresponding to the clear-water scour condition of the approaching flow velocity. The experiments were run until the equilibrium scour depth d_{se} was reached, which was ascertained when the increase in scour rate does not exceed 5% of the pier diameter after 24 h (Melville and Chiew 1999). Afterward the flow rate was gradually decreased and the sediment recess was drained out slowly so as to avoid the disturbance in the scour hole. Different pier diameters D, foundation diameters D^* (with D/D^* ratios of 0.4 and 0.7), and depth of the top level of foundation below the initial bed level Z are being used in the experimentation. The details of the experimental scheme and results are furnished in Table 1. Also, the experimental data of Melville and Raudkivi (1996) with the scour evolution records are included in Table 1 for comparison. It is important to mention that Melville and Raudkivi (1996) used quartz sand with d_{50}=0.80 mm in their experiments.

Furthermore, the experiments were also conducted for the unsteady-flow conditions in the same recirculating flume with same sediment of median size d_{50}=0.52 mm. The pier diameter D and foundation diameter D^* used were, respectively, 50 and 70 mm. Two different depths of the top level of foundation below initial bed level, Z=10 and 20 mm, were used. Three types of flood hydrographs having the same base period and same peak flow (U/U_c=0.9) but different shapes, as shown in Fig. 1, were considered in this study. Hydrograph Type I is of advanced type having a steep rising limb and flat recession limb while Type III is reverse of Type I (delayed hydrograph). On the other hand, Hydrograph Type II is symmetrical. Unsteady uniform flow was developed by regulating the inlet valve and the tailgate simultaneously, and the desired stepwise hydrographs were attained. However, the range of the flow intensity (U/U_c) for all runs under each step was between 0.65 and 0.9 so that the flow was always at clear-water condition (U/U_c<1). Total six experiments were conducted (two under each hydrograph) and the details are given in Table 2.

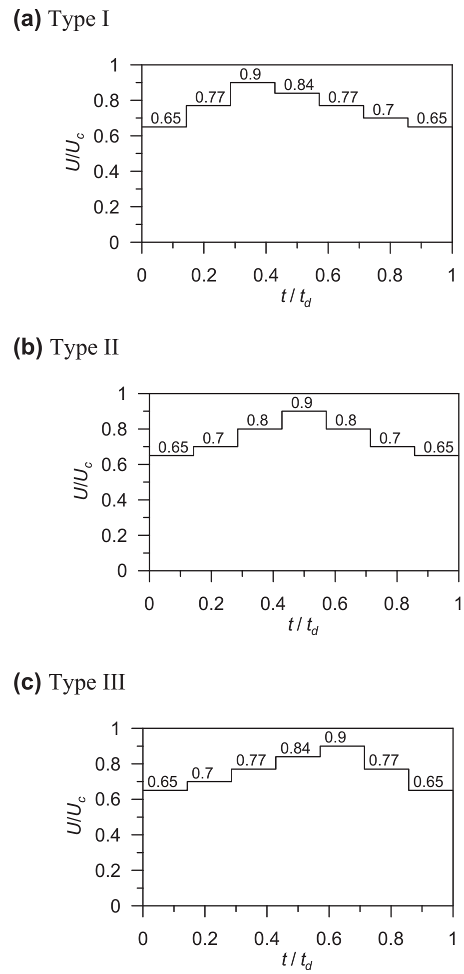

Fig. 1. (a) Schematic diagram showing different zones of scour hole at nonuniform pier (pier with a foundation); (b) temporal variation of scour depth at nonuniform pier; and (c) uniform pier scour with effective pier diameter for computing evolution of scour depth in Zone 3

Steady Flow

Scouring Process and Scour Zones

Based on the pier diameter D, approaching flow depth h, approaching flow intensity (U/U_c), and sediment size d_{50}, the development of scour hole can be divided into three zones, as shown in Fig. 2(a). For small pier sizes and low flow depths, the equilibrium scour-depth hole may occur in Zone 1 with equilib-

Table 2. Experimental Data under Unsteady-Flow Conditions

Hydrograph type	Run	Z (mm)	h (mm)	U/U_c (—)	t_d (min)	Observed d_s (mm)	Computed d_s (mm)
Type I	U1	10	179–204	0.65–0.9	420	46	45.9
	U4	20	179–204	0.65–0.9	420	45	41.8
Type II	U2	10	179–204	0.65–0.9	420	46	47.0
	U5	20	179–204	0.65–0.9	420	42	42.7
Type III	U3	10	179–204	0.65–0.9	420	47	49.9
	U6	20	179–204	0.65–0.9	420	43	45.2

Note: For all the runs, pier diameter D=50 mm and foundation diameter D^*=70 mm.

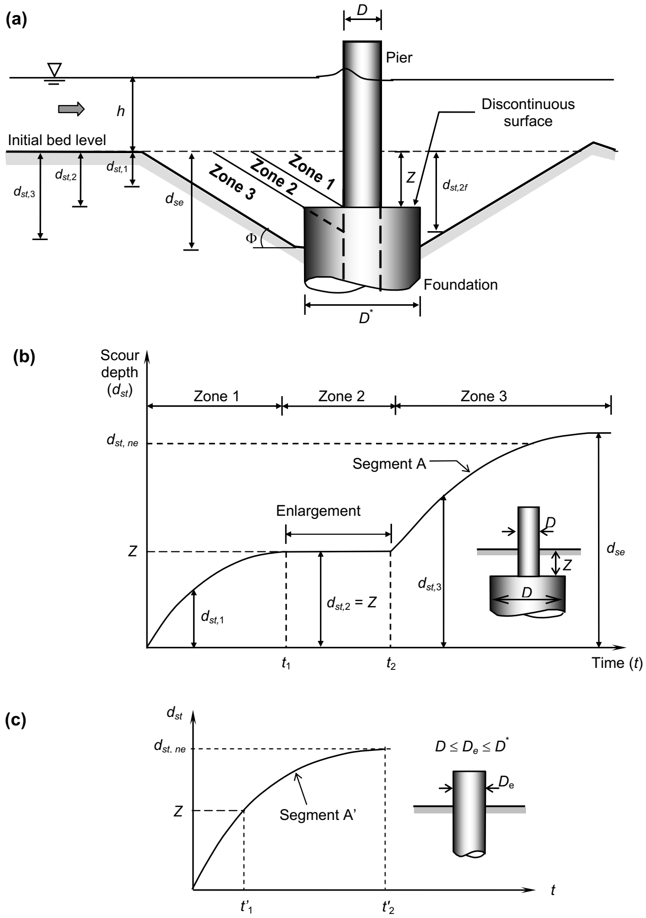

Fig. 2. Pictures showing different stages of the scour process: (a) initial stage; (b) scour in Zone 1; (c) exposure of foundation; (d) scour in Zone 2; (e) scour in Zone 3; and (f) equilibrium scour hole

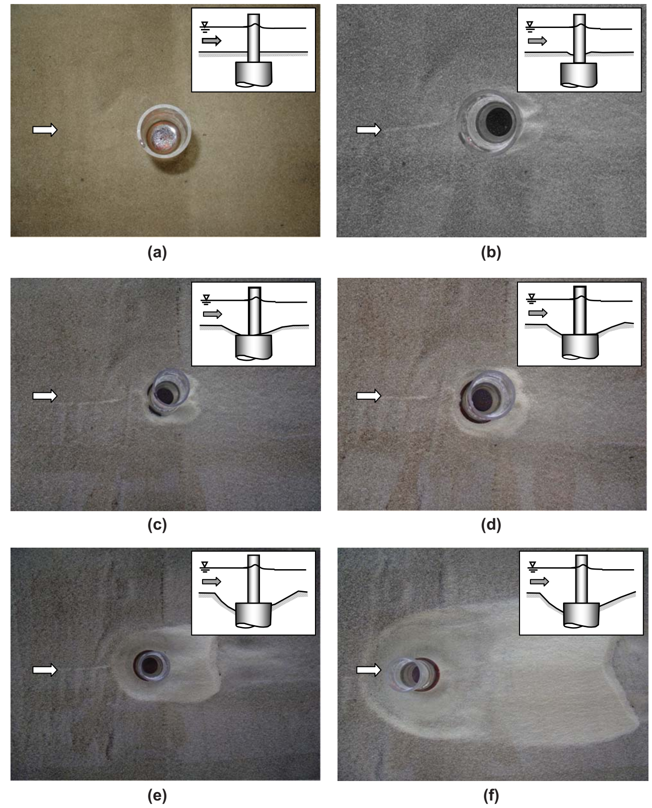

Fig. 3. Comparison of the simulated and measured temporal variations of scour depth for uniform piers under steady-flow conditions

rium scour depth d_{se} being lesser than the depth of the top level of foundation below the initial bed level Z. This occurs when the depth of the top level of foundation below the initial bed level Z is greater than the maximum equilibrium scour depth d_{sm} (that is, $Z > d_{sm}$), the maximum equilibrium scour depth being considered as 2.4 times the pier diameter (2.4D, Melville and Raudkivi 1996). The instantaneous scour depth d_{st} in this zone is considered as $d_{st,1}$ [see Fig. 2(a)]. If the scouring progresses beyond the limit of $d_{st}=Z$ depending on the pier dimensions and flow characteristics, then the instantaneous scour depth $d_{st,2}$ remains constant at Z, which is represented as Zone 2. However, the scour hole gets enlarged. On the other hand, the further scouring that occurs generally for large piers and high flow depths (which occur in all practical cases), the foundation gets exposed. This zone is considered as Zone 3 in which the foundation diameters D^* influence the scour phenomena. The instantaneous scour depth in this zone is assumed as $d_{st,3}$, as illustrated in Fig. 2(a). The temporal variation of scour depth indicating all three zones is shown in Fig. 2(b). In the present study, the emphasis is given to the effect of nonuniform pier size. However, the value of Z in the experimental models is kept less than 2.4D.

In addition, the pictures shown in Figs. 3(a–f) illustrate the temporal evolution of scour hole at nonuniform pier under steady-flow condition obtained in the experimental run. Fig. 3(a) shows the initial plain bed prepared for the experimental run. As the scour initiates corresponding to the clear-water scour condition set for the flow, the scour at pier occurs as if it is a uniform pier of diameter D. This indicates scour in Zone 1 [Fig. 3(b)]. With the increase in scour depth corresponding to the flow potential, the scour depth reaches the top level of the pier foundation at which $d_{st}=Z$. Consequently the foundation gets exposed, as illustrated in Fig. 3(c). Furthermore increase in scour enlarges the dimensions of the scour hole, however, keeping the scour depth constant at Z. The scour process during this period is represented as Zone 2 [see Fig. 3(d)]. After the scour depth d_{st} exceeds the value Z, the scour occurs at pier with its diameter as D^* influencing the scour and is classified as Zone 3 [Fig. 3(e)]. Fig. 3(f) shows the scour hole at equilibrium stage.

Development of Simulation Model

The mathematical model for the temporal variation of scour depth at the nonuniform pier was developed using the concept of the horseshoe vortex being the primary cause for the scouring mechanism (Melville 1975; Kothyari et al. 1992; Dey 1999) along with the consequent decrease in the bed-shear stress with time and volumetric sediment transport theory of Yalin (1977). The semi-empirical model proposed by Mia and Nago (2003) to compute the time variations of scour at uniform piers is modified to describe the scour rate ahead of the pier nose for a nonuniform pier under the steady clear-water scour conditions. As illustrated previously, the scouring process is different for the uniform and nonuniform piers, the model proposed in the present study mainly developed to estimate the scour depth ahead of a nonuniform pier.

Primary Vortex and Bed-Shear Velocity Variations

The diameter of the horseshoe vortex D_v, which is responsible for the initiation of scour, is expressed using the equation of Kothyari et al. (1992) as

$$D_v = 0.28h(D/h)^{0.85} \tag{1}$$

Considering the shape of the scour hole on the upstream side of the pier as an inverted cone with its slant side making an angle Φ called dynamic angle of repose of sediment, the cross-sectional area of the primary vortex at any time t can be expressed as

$$A_t = 0.25\pi D_v^2 + 0.5d_{st}^2/\tan\Phi \tag{2}$$

According to Chiew (1995), the value of the bed-shear velocity located on the initial flat bed where scouring was first observed was $3.3u_*$ (where u_*=shear velocity of approach flow). It decreases as the scour progresses due to an increase in the cross-sectional area of the primary vortex. Following the procedure adopted by Mia and Nago (2003), the instantaneous bed-shear velocity at pier nose u_{*t} can be estimated as

$$u_{*t} = 3.3u_*(0.25\pi D_v^2/A_t)^C \tag{3}$$

where C=exponent estimated to be 0.29 in Zones 1 and 2 by the experimental data.

Volumetric Sediment Transport Rate at Piers

According to Mia and Nago (2003), the sediment transport rate at the pier nose can be described using the bed-load transport function proposed by Yalin (1977), which accounts for the volume of the scour hole developed with time around the pier. The dimensionless sediment transport rate can be expressed as

$$\prod q_{st} = ks_t\left[1 - \frac{\ln(1 + as_t)}{as_t}\right] \tag{4}$$

where q_{st}=volumetric sediment transport rate per unit movable width of scour hole; $\Pi q_{st}=q_{st}/(d_{50}u_{*t})$; k=constant determined by experimental results; s_t=excess dimensionless instantaneous tractive force $(u_{*t}/u_{*c})^2-1$; $a=2.45(\theta_c)^{0.5}/s^{0.4}$; θ_c=Shields parameter $(u_{*c})^2/(\Delta g d_{50})$; $\Delta=s-1$; $s=\rho_s/\rho$; g=gravitational acceleration; ρ_s=mass density of sediment; and ρ=mass density of water.

Mia and Nago (2003) considered the excess dimensionless instantaneous tractive force s_t as $(u_{*t}/u_{*c}-1)$. However, the value of s_t is $(u_{*t}/u_{*c})^2-1$. Accordingly, the value of k=1.8 as suggested by Mia and Nago (2003) is corrected. From the experimental data of the current study, the value of k can be expressed as

$$k_{\text{Zone }1} = \exp\left[1.4\left(\frac{U}{U_c}\right) - 2.6\left(\frac{Z}{D}\right) + 6.1\left(\frac{Z}{D}\right)^2 - 2.7\left(\frac{Z}{D}\right)^3 - 0.16\left(\frac{Z}{D}\right)^4 - 0.18\left(\frac{D^*}{d_{50}}\right)^{0.5}\right] \tag{5}$$

Although the scour phenomenon in Zone 1 is similar to the pier scour for a uniform pier of diameter D, it differs especially when the scour depth approaches the top level of the pier foundation. The pier foundation somehow causes a retardation effect on the downflow. It may due to the interference of the top surface of the pier foundation to the horseshoe vortex. Therefore, both Z and D^* are included in Eq. (5) to incorporate this effect. For any number of time step n, the volume of the scour hole per unit movable width at any time q_{vt} can be expressed as $q_{vt}=\sum_{i=0}^{n} q_{st_i}$, where

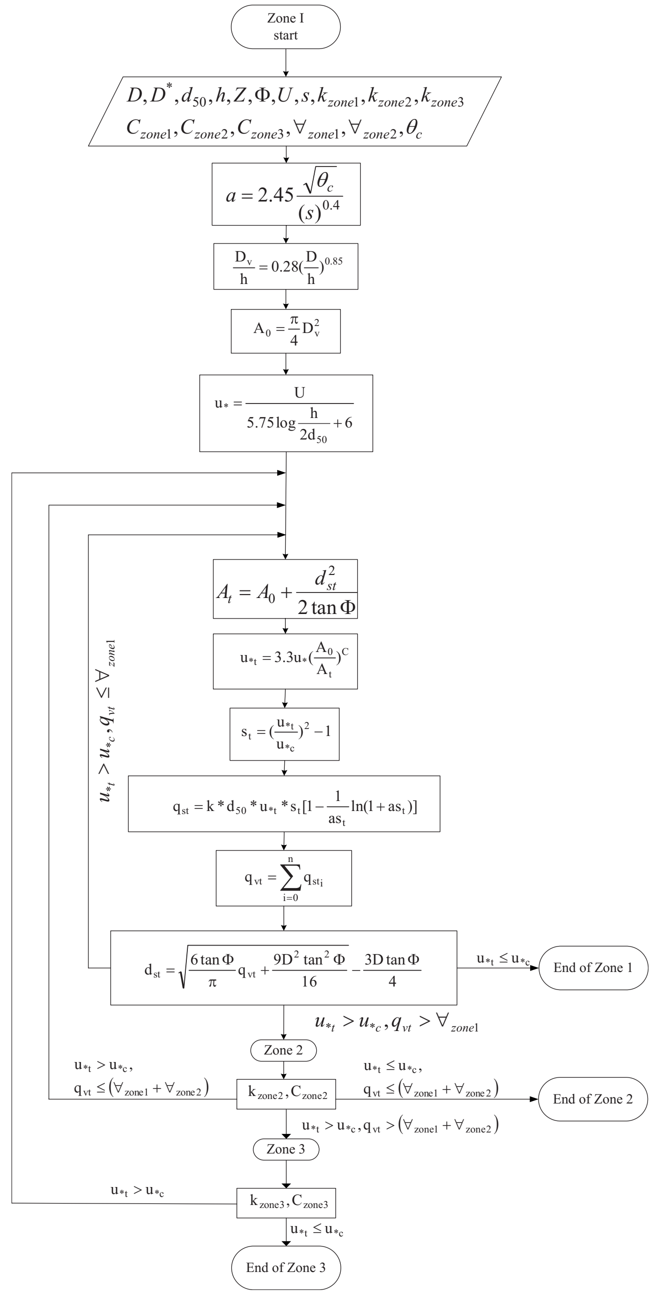

Fig. 4. Temporal variation of scour depth for nonuniform piers (calibration using data of the present study)

i=time step index. Assuming that the shape of the scour hole remains constant with its shape as an inverted cone during the scouring process, the scour depth at time t can be expressed as

$$d_{st} = \sqrt{\frac{6\tan\Phi}{\pi}q_{vt} + \frac{9D^2\tan^2\Phi}{16}} - \frac{3D\tan\Phi}{4} \tag{6}$$

Eq. (6) is used to estimate the scour depth in Zone 1, which is similar to the uniform pier condition. When the scour depth reaches Z, the scouring process enters Zone 2.

In fact, in Zone 2, the horseshoe vortex causes the enlargement of the scour hole; however, the scour depth remains unchanged as $d_{st}=d_{st,2}=Z$. To incorporate the retardation effect of the discontinuous surface, the value of k in Yalin (1977) equation was modified based on the experimental data collected in the present study and those of Melville and Raudkivi (1996) as

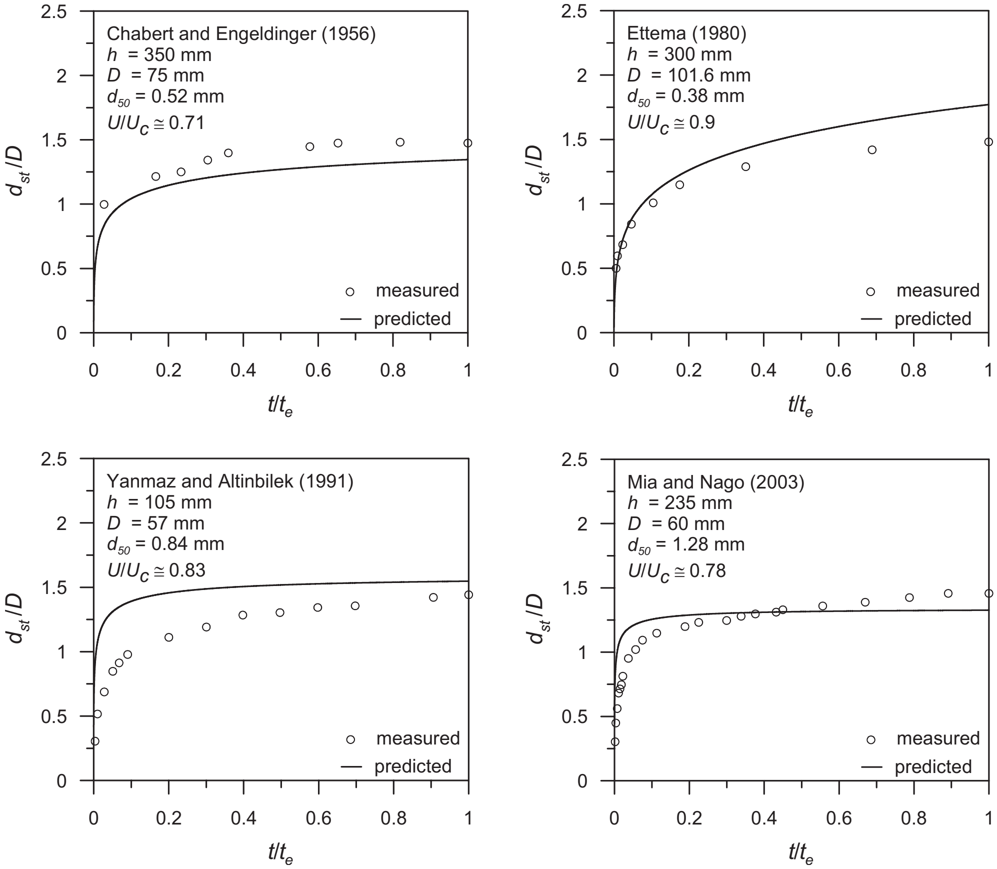

Fig. 5. Temporal variation of scour depth for nonuniform piers (calibration using data of Melville and Raudkivi 1996)

$$k_{\text{Zone }2}=\exp\left[13.2\left(\frac{U}{U_c}\right)+0.56\left(\frac{Z}{D}\right)+0.22\left(\frac{D^*}{d_{50}}\right)-3.7\left(\frac{D^*}{d_{50}}\right)^{0.5}\right] \tag{7}$$

Eq. (7) indicates that $k_{\text{Zone }2}$ decreases with an increase of parameters Z/D and D^*/d_{50}, respectively. Since the volumetric sediment transport rate q_{st} is proportional to k, physically the time to reach Zone 3 from Zone 2 decreases with an increase in the value of $k_{\text{Zone }2}$.

For calculation purpose, $d_{st,2}$ is assumed to be a variable which increases with an increase of the scouring volume. When the final scour depth in Zone 2 corresponding to the bottom of the scour hole on the upstream side touching the edge of the foundation $d_{st,2}$ [see Fig. 2(a)] reaches a value of $d_{st,2f}$ $[=Z+0.5(D^*-D)\tan\Phi]$, the scour depth enters into Zone 3. In Zone 3, the horseshoe vortex gets affected by the discontinuous surface for which a scheme is herein proposed to compute the temporal evolution of the scour depth. As shown in Fig. 2(b), the scour depth evolves from the value of Z to $d_{st,ne}$ (where $d_{st,ne}$=instantaneous scour depth at nonuniform pier with effective pier diameter D_e) along Segment A in Zone 3 with a nonuniform pier.

Melville and Raudkivi (1996) proposed a method of using an effective pier diameter D_e in estimating the scour depth for nonuniform cylindrical pier. This concept is adopted in the present study to compute the scour depth in Zone 3. To determine the equilibrium scour depth, Segment A in Fig. 2(b) is assumed to be equivalent to Segment A′ in Fig. 2(c) for a uniform pier with an effective pier diameter D_e. However, Melville and Raudkivi (1996) indicated that the use of D_e leads to conservative estimate of scour depth for nonuniform cylindrical piers. Therefore, exponent C in Eq. (3) requires modification to reflect the scouring process in Zone 3. From the experimental data of Melville and Raudkivi (1996) and present study, the regression equation for exponent C in Zone 3 is developed as

$$C_{\text{Zone }3}=\exp\left[0.43\left(\frac{U}{U_c}\right)-1.4\left(\frac{Z}{D}\right)-0.17\left(\frac{D^*}{d_{50}}\right)^{0.5}+0.014\left(\frac{Z}{D}\right)\left(\frac{D^*}{d_{50}}\right)\right] \tag{8}$$

In fact, the time to equilibrium decreases with an increase in value of C for Zone 3. The computation of temporal variation of scour depth at nonuniform cylindrical pier with an unexposed foundation is given as a flowchart in Fig. 4.

Validation of Model

Initially, the coefficients k and C are determined using some randomly selected experimental data (present study—Runs S5, S6, S9, and S10) and two data sets (MR-D1 and MR-D2) of Melville and Raudkivi (1996). The value of k for Zone 1 can be obtained from Eq. (5) and for Zones 2 and 3 from Eq. (7). On the other hand, C=0.29 in Zones 1 and 2, while its value can be calculated from Eq. (8) for Zone 3. As mentioned before, the scour behavior in Zone 1 is similar (but not identical) to the pier scour for a uniform pier. The suitability of the model is first compared with uniform pier cases using existing experimental data under the steady clear-water scour condition by assuming that Z=0 and D^*=D in Eq. (5). Fig. 5 shows a comparison of the simulated and measured temporal variation of scour depth for randomly selected

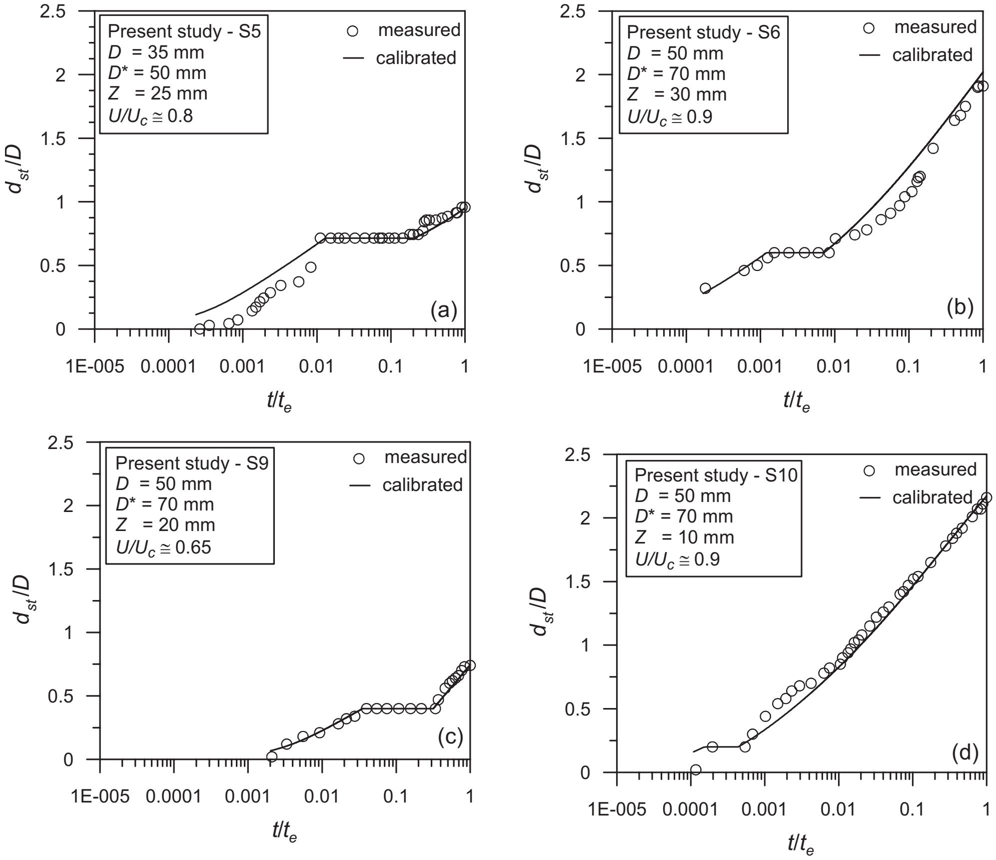

Fig. 6. Temporal variation of scour depth for nonuniform piers (prediction using data of the present study)

experimental data of Chabert and Engeldinger (1956), Ettema (1980), Yanmaz and Altinbilek (1991), and Mia and Nago (2003) with U/U_c=0.7–0.9. The results show that the simulated temporal variation of scour depth by the present model is acceptable. However, it has to be pointed out that uniform pier scour data were not included in the regression analysis in Eq. (5). Therefore, in general, Eq. (5) is not recommended for simulating the temporal variation of scour depth for uniform pier cases. Instead, one may use those models developed mainly for the simulation of uniform pier scour, e.g., Oliveto and Hager (2005).

Fig. 6 shows the variation of dimensionless scour depth d_{st}/D with dimensionless time t/t_e for the calibration runs S5, S6, S9, and S10. Although there exist certain discrepancy between the experimental data and the simulated results during the initial scouring stage, in general, the model describes the scouring processes in Zones 2 and 3 reasonably well. Similarly, Fig. 7 shows the time variation of scour depth with time for the calibration runs (MR-D1 and MR-D2) of Melville and Raudkivi (1996). The model results are in good agreement with the experimental data. Hence this confirms the calibration of the model.

Moreover, the validity of the model is tested with the chosen remaining experimental data, which were not included in the development of the empirical formulas for k and C [Eqs. (5), (7), and (8)]. Fig. 8 shows the dependency of dimensional scour depth d_{st}/D on dimensionless time t/t_e for the present experimental runs S3, S7, S8, and S11 and Fig. 9 for the data (MR-D3) of Melville and Raudkivi (1996). As the experimental data available for the estimation of coefficients k and $C_{\text{Zone 3}}$ are limited, some discrepancies between the measured and predicted values can be detected. However, in general, the model predicts the time evolutions of the scour depth reasonably well for both uniform and nonuniform piers with unprotruding foundations.

The comparison of dimensionless equilibrium scour depths d_{se}/D computed from the present model with the present experimental data and data of Melville and Raudkivi (1996) is shown in Fig. 10. The correlation coefficient being 0.972 between the computed and experimental data indicates that the model fits very well with the experimental data.

Unsteady Flow

Many researchers have reported that the failures of cross-river bridges mainly occur during floods. The scouring process during a flood is totally different from that under steady-flow conditions. Because during floods, the bridge piers get exposed to flood hydrographs having varying flow conditions. Hence, it is very important to investigate the scouring process during unsteady flows. Briaud et al. (2001) proposed the SRICOS method (prediction of scour rate in cohesive soils at bridge piers) to calculate the scour depth due to the multiple flood events at uniform piers. Chang et al. (2004) and Oliveto and Hager (2005) used the similar concept to calculate the temporal variation of pier scour depth under unsteady flows at uniform piers. However, as is mentioned earlier, the bridge piers frequently behave as nonuniform piers depending on the exposure of their foundation. Therefore, in this study, a scheme based on the superposition concept is proposed to calculate the time variations of pier scour at nonuniform piers under unsteady-flow conditions.

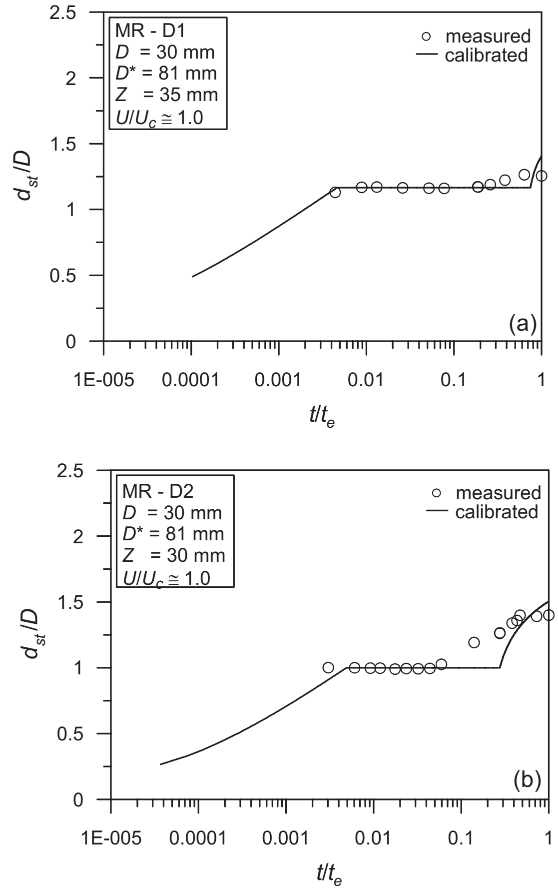

Fig. 7. Temporal variation of scour depth for nonuniform piers (prediction using data of Melville and Raudkivi 1996)

The scheme used in computing the temporal evolution of scour depth at a nonuniform pier under unsteady-flow conditions is schematically depicted in Fig. 11. To illustrate the procedure, the symmetrical stepwise hydrograph of Type II [Fig. 11(a)] is considered, which consists of four steps with discharge rates Q_1 (for duration t_1), Q_2 (for duration t_1-t_2), Q_3 (for duration t_2-t_3), and Q_4 (for duration t_3-t_4). Only rising part of the hydrograph is considered because once the flow rate starts decreasing, the scour depth usually remains constant at its maximum value. Fig. 11(b) shows the temporal evolution of scour-hole volume $\forall_{st}$ for different steady-flow rates (Q_j, $j=1-4$) considered independently for a uniform pier. For the case of stepwise flood hydrograph the variation of scour-hole volume $\forall_s$ with time t is described as follows:

- During the first flow rate Q_1 for time interval up to t_1, the variation of scour-hole volume $\forall_{st}$ follows the $\forall_{st}$ curve of Q_1 (that is, Curve 0A). The corresponding scour-hole volume is $\forall_{s1}$.
- When the flow rate increases from Q_1 to Q_2 at time t_1, the temporal evolution of scour-hole follows Path A′B of the $\forall_{st}$ curve corresponding to Q_2 because time required for the scour-hole volume to reach $\forall_{s1}$ under flow rate Q_2 ($>Q_1$) is lesser than t_1. This time is indicated as t_2^1 in Fig. 11(b).
- As the flow rate increases from Q_2 to Q_3 ($>Q_2$) corresponding to time $t=t_2^1+(t_2-t_1)$, the $\forall_{st}$ curve follows Path B′C of the $\forall_{st}$ curve of Q_3 as the scour-hole volume becomes $\forall_{s2}$. Here (t_1-t_2) represents the duration of flow rate Q_2. The same procedure continues for the remaining steps of hydrograph.

Fig. 11(c) demonstrates the temporal evolution of scour-hole volume $\forall_{st}$ for a uniform pier under unsteady-flow conditions. The curve follows Path 0ABCD. A similar procedure is followed by Chang et al. (2004) and Oliveto and Hager (2005) considering the temporal evolution of scour depth at a uniform pier under unsteady flow. Following the same procedure, the temporal evolution of scour-hole volume $\forall_{st}$ for the nonuniform pier is obtained. Fig. 11(d) illustrates the temporal evolution of scour-hole volume $\forall_{st}$ for different steady-flow rates (Q_j, $j=1-4$) considered independently for a nonuniform pier. The variation of $\forall_{st}$ with time t for a nonuniform pier derived from Fig. 11(d) is presented in Fig. 11(e). The scour-hole volume $\forall_{st}$ is then used to calculate the scour depth at nonuniform bridge pier. Fig. 11(f) shows the temporal variation of scour depth d_{st} with time t for nonuniform pier under unsteady-flow condition. The curve of d_{st} follows Path $0A_1B_1C_1D_1E_1$. It is important to mention that the exact positions of the end of Zones 1 and 2 depend on the value of d_{st} and Z. Nevertheless, Fig. 11(f) shows a typical variation.

The simulation model developed was run incorporating the methodology described above for the present experimental data to obtain temporal evolution of scour volume $\forall_{st}$ and scour depth d_{st} under stepwise hydrographs. The simulated results obtained by the model showing the variations of scour volume $\forall_{st}$ and scour depth d_{st} with time t together with the experimental data are represented in Fig. 12. The results obtained from the model show good agreements with experimental results, as can be seen in Fig. 12. Even though there are some discrepancies between the predicted and experimental results in Zone 1 for all three types of stepwise hydrographs, the proposed model predicts the scour-depth evolutions for Zones 2 and 3 reasonably well. On the other hand, during the flood recession, the scour depth usually does not increase with time, and the present model can predict it very well. Hence, it indicates that the proposed model may be well applied to predict the temporal evolution of scour depths of nonuniform piers with unexposed foundations under unsteady flows.

The comparison of dimensionless maximum scour depth d_{sm}/D under unsteady-flow conditions computed from the present model with the experimental data is shown in Fig. 13. Two dashed lines with discrepancy ratios (ratio of computed to obtained values) of 1.05 and 0.95 are also plotted for reference. The correlation coefficient being 0.988 for the computed and experimental data implies that the proposed model corresponds reasonably well with the experimental data.

Conclusions

The effects of foundation geometry and unsteady flow on the scour depth at the nonuniform piers with unexposed foundation were investigated through laboratory experiments and the simulation by a semiempirical model based on the concept of primary vortex and the volumetric rate of sediment transport. For the simulation of the scour-depth evolution, initially, empirical formulas for the estimation of the sediment transport rate coefficient k and the scouring rate coefficient C in Zones 1–3 were developed using randomly selected laboratory experimental data of the present study and Melville and Raudkivi (1996) data. A concept of superposition using an effective pier diameter was then applied to simulate the scouring process for Zone 3.

For the steady-flow condition, in general, the proposed model predicted the temporal evolution of scour depth reasonably well for both uniform and nonuniform piers with unexposed foundations. The equilibrium scour depths predicted by the model are in excellent agreement with the experimental data. The simulation

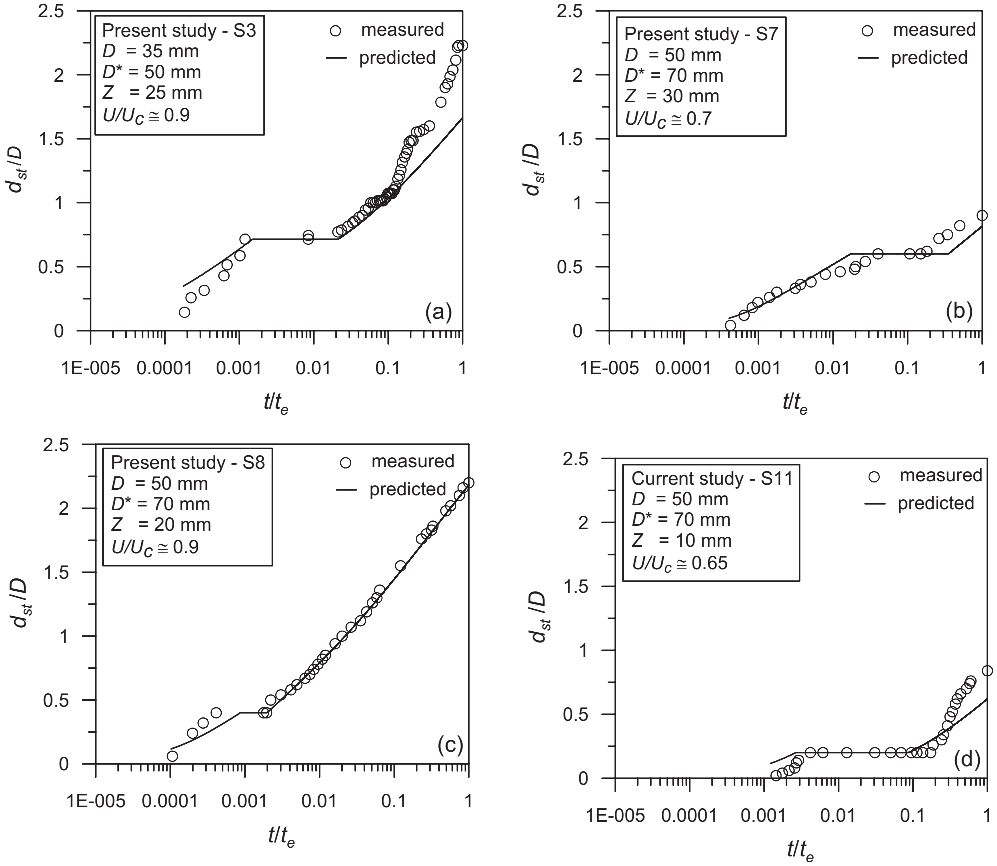

Fig. 8. Dimensionless equilibrium scour depths for nonuniform piers: comparison between the observed and computed values

model is further extended to predict the scour depth at nonuniform piers under unsteady flows including the advanced, symmetrical, and delayed hydrographs. The proposed model yielded reasonably satisfactory results for the temporal evolution of scour depth. The comparison of maximum scour depths obtained by the model and experimental data shows that the model can well be applied (maximum error of $\approx 7\%$) to predict the scour depths at nonuniform piers under unsteady flows. Although the model is limited to the clear-water scour conditions, it can be used as a

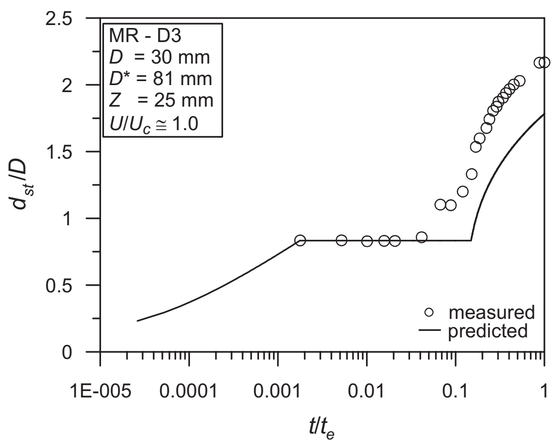

Fig. 9. Illustrative scheme for computing scour-depth evolution under stepwise hydrograph at nonuniform pier: (a) Hydrograph Type II considering only rising portion; (b) variation of $\forall_s$ with t for different steady flows for uniform pier; (c) variation of $\forall_s$ with t for uniform pier under stepwise hydrograph; (d) variation of $\forall_s$ with t for nonuniform pier under stepwise hydrograph; (e) variation of $\forall_s$ with t for unsteady-flow-nonuniform pier; and (f) variation of d_s with t for unsteady-flow-nonuniform pier

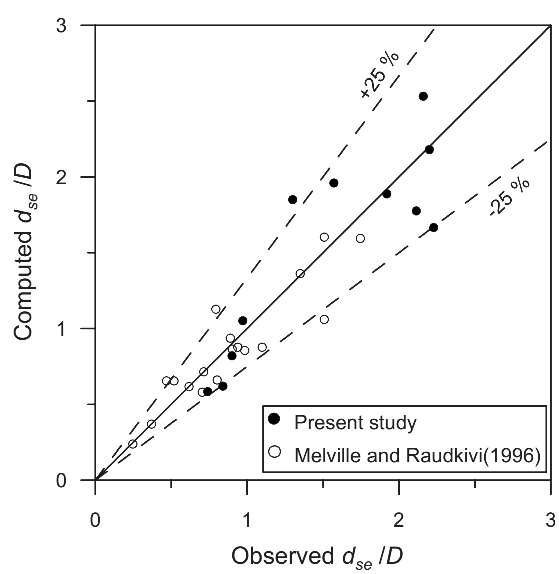

Fig. 10. Simulated and measured dimensionless scour-depth evolutions under stepwise hydrographs (with $D = 50$ mm and $D^* = 70$ mm)

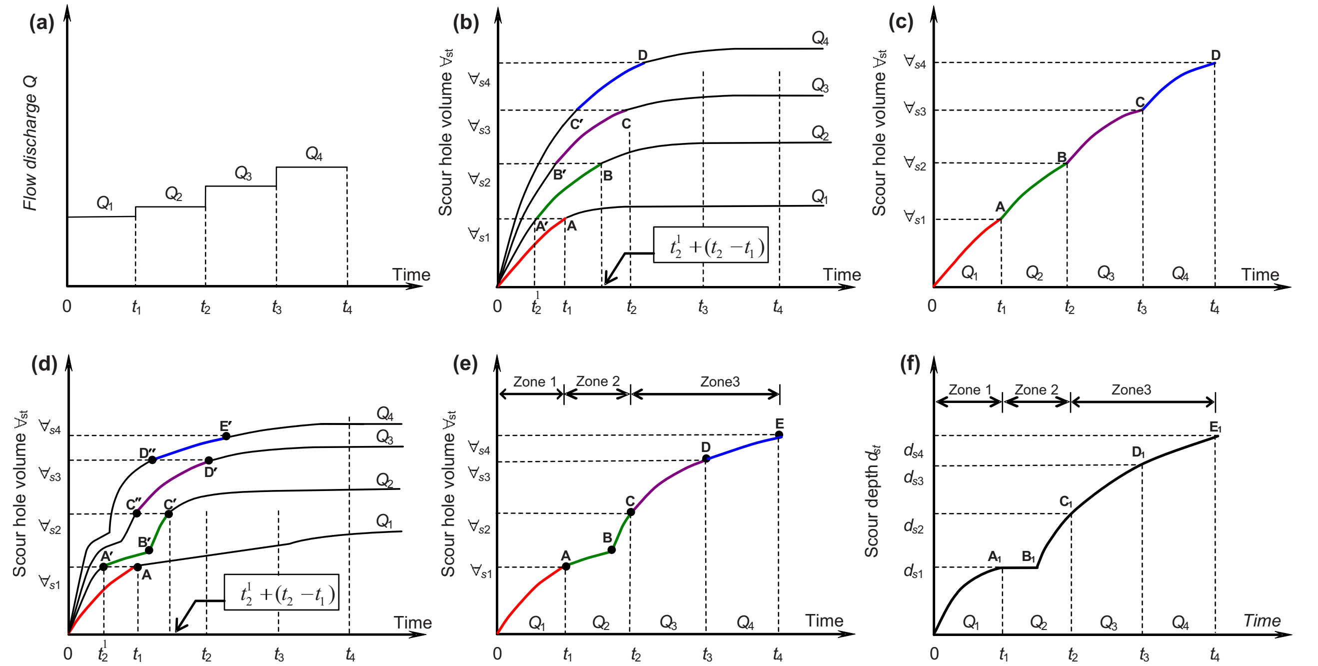

Fig. 11. Dimensionless maximum scour depths under unsteady-flow conditions for nonuniform piers: comparison between the observed and computed values

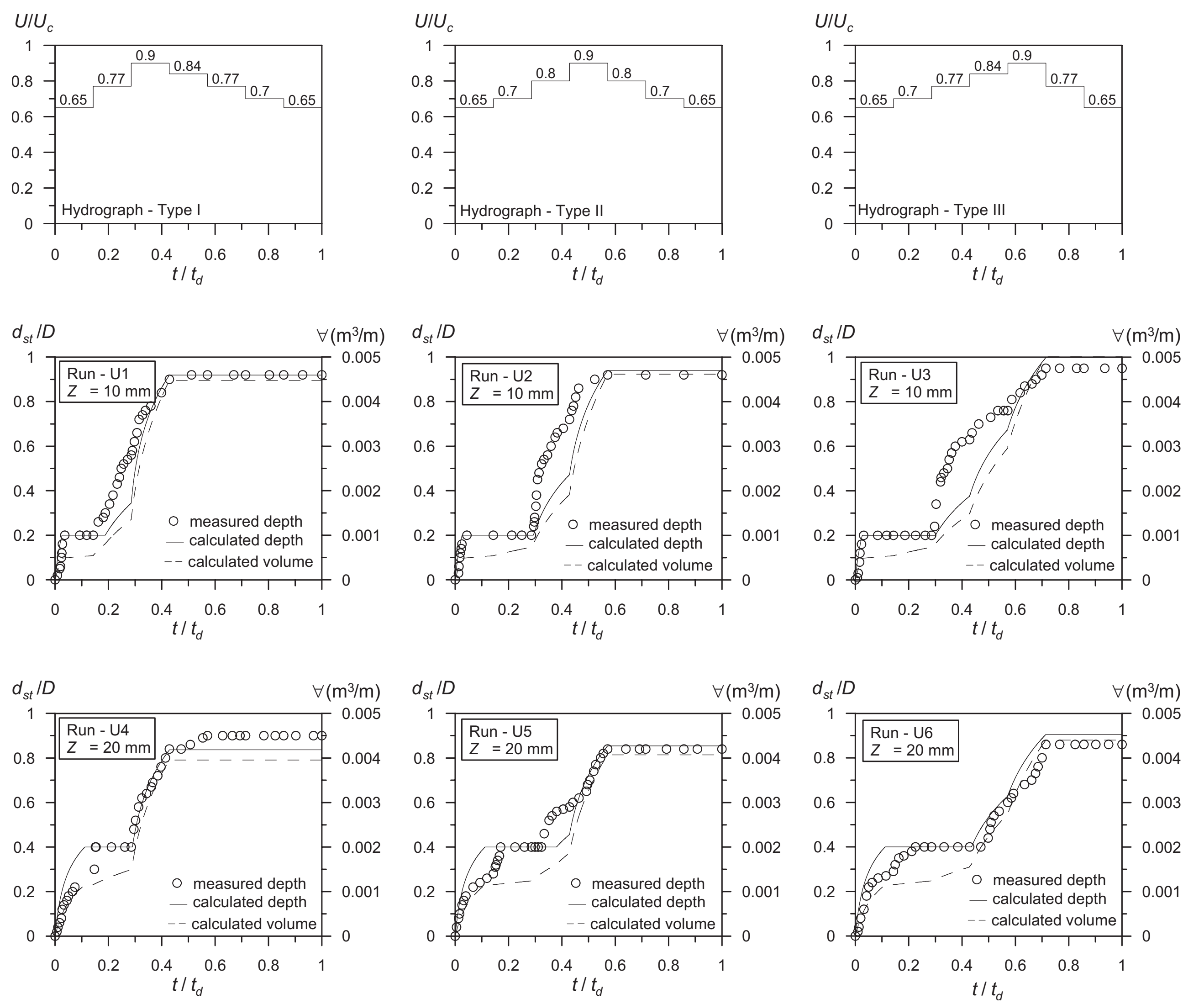

Fig. 12. Simulated and measured dimensionless scour-depth evolution under stepwise hydrographs (with $D=50$ mm and $D^{*}=70$ mm)

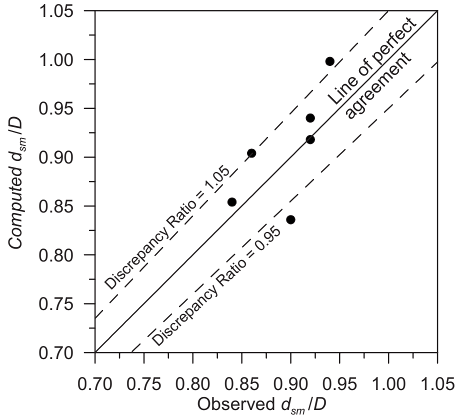

Fig. 13. Dimensionless maximum scour depths under unsteady flow conditions for nonuniform piers: comparison between the observed and computed values

reference guide for the bridge closure where the bed level does not significantly vary with flow.

Acknowledgments

The research is supported by the National Science Council of the R.O.C. The writers would like to thank Mr. Tien-Feng Chang and Mr. Ming-Cheng Peng of National Chung Hsing University for their technical assistance during the experiments.

Notation

The following symbols are used in this paper:

A_t = cross-sectional area of primary vortex at time t (L^2);
A_0 = Initial cross-sectional area of primary vortex (L^2);
a = $2.45(\theta_c)^{0.5}/s^{0.4}$ (−);
C = scouring rate coefficient (−);
D = pier diameter (L);
D_e = effective pier diameter (L);
D_v = diameter of horseshoe vortex (L);
D^* = foundation diameter (L);
d_s = scour depth (L);
d_{se} = equilibrium scour depth (L);
d_{sm} = maximum scour depth (L);
d_{st} = instantaneous scour depth (L);
$d_{st,ne}$ = instantaneous scour depth at nonuniform pier with effective pier diameter (L);
d_{50} = median size of sand (L);
g = gravitational acceleration ($L\,T^2$);
h = approaching flow depth (L);
i = step number (−);
j = number of flow rates (−);
k = sediment transport rate coefficient (−);
n = time step (−);
Q = flow discharge ($L^3\,T^{-1}$);
Q_j = jth discharge of stepwise hydrograph ($L^3\,T^{-1}$);
q_{st} = volumetric sediment transport rate per unit movable width of scour hole at time t ($L^2\,T^{-1}$);
q_{vt} = volume of scour hole per unit width at time t ($L^3\,T^{-1}$);
s = relative density of sediments (ρ_s/ρ) (−);
s_t = excess dimensionless tractive force at time t (−);
t = time (T);
t_d = duration of hydrograph (T);
t_e = equilibrium time of scour (T);
U = average approaching flow velocity ($L^2\,T^{-1}$);
U_c = critical velocity ($L\,T^{-1}$);
u_* = shear velocity in approaching flow ($L\,T^{-1}$);
u_{*c} = critical shear velocity ($L\,T^{-1}$);
u_{*t} = instantaneous shear velocity at pier nose ($L\,T^{-1}$);
Z = depth of the top level of foundation below initial bed level (L);
$\forall_s$ = volume of scour hole (L^3);
$\forall_{st}$ = volume of scour hole at any time t (L^3);
$\Delta = s-1$ (−);
θ_c = Shields parameter (−);
ρ = mass density of water (ML^{-3});
ρ_s = mass density of sediment (ML^{-3});
σ_g = geometric standard deviation of sediment size distribution (−); and
Φ = angle of repose of sediment (−).

Subscripts

1, 2, 3 = Zone 1, Zone 2, and Zone 3.

References

Breusers, H. N. C., Nicollet, G., and Shen, H. W. (1977). "Local scour around cylindrical piers." *J. Hydraul. Res.*, 15(3), 211–252.

Breusers, H. N. C., and Raudkivi, A. J. (1991). *Scouring. IAHR hydraulic design manual 2*, Balkema, Rotterdam, The Netherlands.

Briaud, J. L., Chen, H. C., Kwak, K. W., Han, S.-W., and Ting, F. C. K. (2001). "Multiflood and multilayer method for scour rate prediction at bridge piers." *J. Geotech. Geoenviron. Eng.*, 127(2), 114–125.

Chabert, J., and Engeldinger, P. (1956). "Etude des affouillements autour des piles de ponts. Serie A." *Laboratoire National d'Hydraulique*, Vol. 6, Quai Watier, Chatou, France (in French).

Chang, W. Y., Lai, J. S., and Yen, C. L. (2004). "Evolution of scour depth at circular bridge piers." *J. Hydraul. Eng.*, 130(9), 905–913.

Chiew, Y. M. (1984). "Local scour at bridge piers." *Rep. No. 335*, School of Engineering, The Univ. of Auckland, New Zealand.

Chiew, Y. M. (1995). "Mechanics of riprap failure at bridge piers." *J. Hydraul. Eng.*, 121(9), 635–643.

Dargahi, B. (1982). "Local scouring around bridge piers—A review of practice and theory." *Bulletin No. 114*, Hydraulic Laboratory, Royal Institute of Technology, Stockholm, Sweden.

Dey, S. (1997a). "Local scour at piers, Part I: A review of development of research." *Int. J. Sediment Res.*, 12(2), 23–46.

Dey, S. (1997b). "Local scour at piers, Part II: Bibliography." *Int. J. Sediment Res.*, 12(2), 47–57.

Dey, S. (1999). "Time-variation of scour in the vicinity of circular piers." *Proc. Inst. Civ. Eng., Waters. Maritime Energ.*, 136, 67–75.

Dey, S., Bose, S. K., and Sastry, G. L. N. (1995). "Clear water scour at circular piers: A model." *J. Hydraul. Eng.*, 121(12), 869–876.

Durand-Claye, A. A. (1873). "Expériences sur les affouillements." *Annales des Ponts et Chaussées*, Ler Sémestre, 467.

Ettema, R. (1980). "Scour at bridge piers." *Rep. No. 216*, School of Engineering, Univ. of Auckland, Auckland, New Zealand.

García, M. H., ed. (2008). "Sedimentation engineering: Processes, measurements, modeling and practice." *ASCE Manuals and Rep. on Engineering Practice No. 110*, ASCE, Reston, Va.

Hoffmans, G. J. C. M., and Verheij, H. J. (1997). *Scour manual*, Balkema, Rotterdam, The Netherlands.

Imamoto, H., and Ohtoshi, K. (1987). "Local scour around a non-uniform circular pier." *Proc., 12th IAHR Congress*, Lausanne, Switzerland, 304–309.

Johnson, P. A., and McCuen, R. H. (1991). "A temporal, spatial pier scour model." *Transportation Research Record 1319*, Transportation Research Board, National Research Council, Washington, D.C.

Keutner, C. (1932). "The flow around bridge piers of different shapes and its effects on the river bed." *U.S. Bureau of Reclamation HYD-19, Translation No. 40*, Denver (in German).

Kothyari, U. C., Garde, R. J., and Ranga Raju, K. G. (1992). "Temporal variation of scour around circular bridge piers." *J. Hydraul. Eng.*, 118(8), 1091–1106.

Melville, B. W. (1975). "Scour at bridge sites." *Rep. No. 117*, School of Engineering, Univ. of Auckland, Auckland, New Zealand.

Melville, B. W., and Chiew, Y. M. (1999). "Time scale for local scour at bridge piers." *J. Hydraul. Eng.*, 125(1), 59–65.

Melville, B. W., and Coleman, S. E. (2000). *Bridge scour*, Water Resources Publications, Highlands Ranch, Colo.

Melville, B. W., and Raudkivi, R. J. (1996). "Effects of foundation geometry on bridge pier scour." *J. Hydraul. Eng.*, 122(4), 203–209.

Mia, M. F., and Nago, H. (2003). "Design method of time-dependent local scour at circular bridge pier." *J. Hydraul. Eng.*, 129(6), 420–427.

Oliveto, G., and Hager, W. H. (2005). "Further results to time-dependent local scour at bridge elements." *J. Hydraul. Eng.*, 131(2), 97–105.

Oliveto, G., Hager, W. H., and Di Domenico, A. (2005). "Additional results on scour at bridge piers." *Proc., 31st IAHR Congress*, Seoul, Korea, 2964–2972.

Richardson, E. V., and Davis, S. R. (2001). "Evaluating scour at bridges." *HEC18 FHWA NHI-001*, Federal Highway Administration, U.S. Dept. of Transportation, Washington, D.C.

Shen, H. W., Ogawa, Y., and Karaki, S. (1965). "Time variation of bed deformation near the bridge piers." *Proc., 11th IAHR Congress*, Leningrad, Russia, 3–14.

Shen, H. W., Schneider, V. R., and Karaki, S. (1969). "Local scour around bridge piers." *J. Hydr. Div.*, 95(6), 1919–1940.

Shirhole, A. M., and Holt, R. C. (1991). "Planning for a comprehensive bridge safety program." *Transportation Research Record 1290*, Transportation Research Board, National Research Council, Washington, D.C., 39–50.

Simons, D. B., and Richardson, E. V. (1966). "Resistance to flow in alluvial channels." *Professional Paper 422J*, USGS, Washington, D.C.

Sumer, B. M., Christiansen, N., and Fredsoe, J. (1992). "Time scale of scour around a vertical pile." *Proc., 2nd Int. Conf. on Offshore and Polar Engineering*, Vol. 3, San Francisco, Calif., 308–315.

Yalin, M. S. (1977). *Mechanics of sediment transport*, Pergamon, New York.

Yanmaz, A. M., and Altinbilek, H. D. (1991). "Study of time-dependent local scour around bridge piers." *J. Hydraul. Eng.*, 117(10), 1247–1268.